American Journal of Pathology, Vol. 148, No. 4, April 1996

Cytoskeletal Changes in Podocytes Associated with Foot Process Effacement in Masugi Nephritis

Isao Shirato,* Tatsuo Sakai,† Kenjiro Kimura,‡ Yasuhiko Tomino,§ and Wilhelm Kriz*

From the Institute of Anatomy and Cell Biology, University of Heidelberg, Heidelberg, Germany, and the First Department of Anatomy‡ and Division of Nephrology,§ Department of Medicine, Juntendo University, School of Medicine, and the Second Department of Internal Medicine,‡ Tokyo University, Tokyo, Japan*

Foot process effacement represents the most characteristic change in podocyte phenotype under a great variety of experimental as well as human glomerulopathies. It consists in simplification up to a total disappearance of an interdigitating foot process pattern. Finally, podocytes affix to the glomerular basement membrane by outspread epithelial sheets. Structural and immunocytochemical techniques were applied to analyze the cytoskeletal changes associated with foot process effacement in Masugi nephritis. Three days after injection of the anti-glomerular-basement-membrane serum an interdigitating foot process pattern was almost fully lost; more than 90% of the outer glomerular capillary surface were covered by expanded sheets of podocyte epithelium that contain a highly organized cytoskeleton adhering to the basal cell membrane. Structurally, this cytoskeleton consists of an interwoven network of microfilaments with regularly distributed dense bodies, which obviously serve as cross-linkers within this network. Immunocytochemically, the expression of actin, α-actinin, and pp44 (a specific podocyte protein normally associated with the cytoskeleton of foot processes) were increased in this structure; α-actinin was especially prominent in the dense bodies. The results are consistent with the view that foot process effacement represents an adaptive change in cell shape including hypertrophy of the contractile apparatus, reinforcing the supportive role of podocytes. Several factors associated with increased distending forces to podocytes may underlie this phenotype change including loss of mesangial support, elevated glomerular pressures, and impairment of GBM substructure as well as of podocyte-GBM-contacts. Twenty-eight days after serum injection a remodeling of the foot process pattern was seen. It appears that this restitution depends on a preceding repair of mesangial support function to glomerular capillaries. (Am J Pathol 1996, 148:1283–1296)

Podocytes when challenged in pathological situations exhibit a series of stereotyped structural changes including hypertrophy, cell body attenuation, pseudocyst formation, foot process effacement, cytoplasmic accumulation of lysosomal elements, and detachments from the glomerular basement membrane (GBM). Cell body attenuation and pseudocyst formation have been shown to result directly from mechanical overextension.[1] Plausible explanations are available for cell hypertrophy (hyperfiltration), accumulation of absorption droplets and lysosomes (uptake and degradation of filtered proteins, most dramatically seen in protein overload proteinuria[2]), and detachments (impairment of cell membrane connections with the GBM[3]). No convincing interpretation is at hand for foot process effacement, which represents a most characteristic change in podocyte cell shape common to a great variety of glomerulopathies. Foot process effacement consists in the gradual simplification of the interdigitating foot process pattern. Instead of foot processes, the outer GBM surface is eventually cov-

Supported by Deutsche Forschungsgemeinschaft grant Kr 546/9–1.

Accepted for publication November 1, 1995.

Address reprint requests to Dr. Isao Shirato, Division of Nephrology, Department of Medicine, Juntendo University, School of Medicine, Tokyo 113, Japan.

ered by rather expanded sheets of thin podocyte epithelium.

This study was undertaken to elucidate in more detail the role of podocytes in the development of focal segmental glomerulosclerosis in Masugi nephritis. As suggested previously,[4] our observations demonstrate that podocytes are decisively involved in sclerosis development; these results will be published elsewhere. The present paper analyzes the deterioration of the filtration surface from a delicate foot process pattern into a coarse cover with epithelial sheets. Making use of improved ultrastructural techniques to display cytoskeletal elements[5] and of immunocytochemical techniques, it is shown that foot process effacement is associated with substantial changes in the cytoskeleton culminating in the development of a prominent mat of densely interconnected microfilament bundles.

Materials and Methods

Animals

Male Sprague-Dawley rats (weighing 150 to 170 g) were obtained from Charles River Japan (Kanagawa, Japan). Animals were kept in an air-conditioned room and maintained on a commercial stock diet and tap water *ad libitum*.

Induction of Masugi Nephritis

Masugi nephritis was induced by a single intravenous injection of rabbit anti-rat-GBM serum (0.1 ml per 100 g body weight). Rabbit anti-rat-GBM serum was kindly provided by Yoshio Suzuki and Tadashi Nagamatsu (Faculty of Pharmacology, Meijo University, Nagoya, Japan). In addition to a control group (no injection), six experimental groups with animals sacrificed 4 hours and 1, 3, 7, 10, and 28 days after the injection were studied. Each group consisted of six rats; four were used for structural studies and two were used for immunocytochemistry. The 4-hour and the 7-day groups consisted of only two rats, which were used for structural studies. One day before sacrifice, all rats (except the 4-hour and 7-day groups) had a 24-hour urine collection to determine total protein excretion. Urinary protein concentration was determined by using the Tonein TP kit (Coomasie brilliant blue G250; Otsuka Pharmacy, Tokyo, Japan).

Fixation of Kidneys

At the time of sacrifice, the kidneys were fixed by total body perfusion as described previously.[6] Briefly, after anesthesia with Nembutal (100 mg/kg body weight), the kidneys were retrogradely perfused via the abdominal aorta for 3 minutes at a pressure of 200 mm Hg without prior flushing of the vasculature.

Light and Electron Microscopy

For structural studies the fixative contained 2% glutaraldehyde in 0.1 mol/L sodium phosphate buffer (PBS) at pH 7.4. After perfusion, slices of the kidneys were immersed in the same fixative overnight. Tissue was then processed in a modified postfixation and staining technique that minimizes treatment with osmium tetroxide and uses tannic acid as a contrast agent for better visualization of cytoskeletal elements.[5,7] All samples were finally embedded in Epon 812 by standard procedures. Semi-thin sections (1 μm) stained with toluidine blue were used for light microscopy and morphometry. Ultrathin sections stained in uranyl acetate and lead citrate were observed in a Phillips EM 301.

Morphometry

Morphometric analysis was carried out with a semiautomatic image analysis system (VIDS IV, Ai Tektron, Duesseldorf, Germany) connected to a Zeiss photomicroscope. Mean glomerular tuft volume (V_T) was determined according to Weibel.[8] For each animal, 60 consecutively encountered glomeruli were analyzed in 1-μm sections. Surface area of the glomerular tufts (A_T) was measured under direct visualization (magnification, $\times$690). V_T was calculated according to the formula $V_T = (\beta/k)\ (A)^{3/2}$ where β = 1.38 (a shape coefficient), k = 1.1 (a size distribution coefficient for spheres), and A = mean A_T.

The degree of foot process effacement was estimated as the fraction of outer capillary surface covered with noninterdigitating podocyte portions. A multipurpose test system[8] was overlaid on light micrographs (final magnification, $\times$1280) of four glomerular profiles per animal, randomly sampled in 1-μm epon sections. Intersections of test lines with a capillary wall either covered by foot processes or by noninterdigitating podocyte portions were evaluated. In each animal, roughly 200 intersection points were considered.

Damage Index

To estimate the degree of glomerular damage, glomerular lesions were scored as follows. In 1-μm epon sections 60 consecutively encountered glomeruli per animal were screened. Pseudocysts, tuft appositions, and tuft adhesion to Bowman's capsule were included in the evaluation in a graded weighing. Glomeruli with pseudocysts only were scored as 1, glomeruli with appositions as 2 (generally containing pseudocysts), and glomeruli with adhesions or segmental sclerosis as 3. The sum of these values in each animal is considered to reflect the degree of damage.

Immunocytochemistry

For immunocytochemistry, kidneys were perfusion fixed (see above) with a fixative containing 2% paraformaldehyde in 0.1 mol/L PBS (pH 7.4). For immunocytochemistry at the light microscopic level, pieces of the right kidney were immediately shock frozen in melting isopentane and stored in liquid nitrogen until sectioning. Frozen sections (5 μm thick) were cut on a Reichert 2800 Frigocut and fixed with ice-cold acetone. Immunostaining was done with the indirect immunofluorescence technique. A monoclonal mouse anti-pp44 antibody[9] and a monoclonal mouse anti-α-actinin antibody (clone BM-75.2, Sigma Chemical Co., St. Louis, MO) were used. Rhodamine phalloidin (Sigma) was used to detect filamentous actin (F-actin). Secondary antibodies were fluorescein isothiocyanate-conjugated goat anti-mouse IgG and IgM (Cappel, Denkendorf, Germany). After blocking with 1% bovine serum albumin in PBS (15 minutes), sections were incubated with primary antibodies or rhodamine phalloidin for 1 hour at room temperature. The antibody against pp44 was used undiluted; the antibody against α-actinin was diluted 1:200 in PBS containing 1% bovine serum albumin. Rhodamine phalloidin was diluted 1:40 in PBS. After immunostaining, the sections were examined by epifluorescence in a Reichert Polyvar microscope and photographed using Kodak Tri-X PAN film.

For immunogold labeling, small pieces from the left kidney were dehydrated in ethanol and embedded in LR-White resin (London Resin Co., Woking, UK) by standard procedures. Ultrathin sections were prepared with a Reichert Ultracut E. Sections were transferred to formvar-coated nickel grids (200 mesh) and processed for postembedding immunoelectron microscopy. After washing with PBS, nonspecific binding sites were blocked with 10% fetal calf serum in PBS containing 10 mmol/L glycine for 1 hour at room temperature. For α-actinin and pp44, the same antibodies as described above were used; to visualize actin, a monoclonal mouse anti-actin antibody was applied (code N 350, Amersham International, Buckinghamshire, UK). Dilutions were as follows: anti-pp44, undiluted; anti-α-actinin, 1:200; and anti-actin, 1:500. Incubation was done overnight at 4°C. After rinsing with PBS containing 0.1% bovine serum albumin, rabbit anti-mouse immunoglobulin (Zymed, Aidenbach, Germany) was applied at 1:50 for 1 hour at room temperature as a bridge, followed by a goat anti-rabbit IgG coupled to 10-nm colloidal gold (Biocell, Marburg, Germany) at 1:100 in PBS containing 0.1% bovine serum albumin. The sections were stained with 2% uranyl acetate for 2 to 5 minutes and were observed with a Phillips EM 301.

Statistics

Results are reported as mean ± standard deviation (SD). Group differences were assessed by one-way analysis of variance followed by Scheffé multiple range test. Correlation analysis between glomerular damage (damage index), tuft volume, and urinary protein excretion was done by Spearman's rank correlation test. All statistical calculations were performed with the SPSS analysis program (Chicago, IL).

Results

The development of the disease as seen in the present experiments was similar to previous studies of Masugi nephritis[10,11] and is documented by various parameters listed in Table 1. Increase in urinary protein excretion and in structural damage were significantly correlated with each other ($r_s = 0.7806$; $P < 0.01$). Up to day 10, a good correlation was also seen between protein excretion as well as damage score on the one hand and tuft hypertrophy on the other hand ($r_s = 0.669$; $P < 0.02$ and $r_s = 0.786$; $P < 0.01$, respectively). Thereafter, tuft volume increased further together with a significant increase in the incidence of sclerosis, whereas the damage index (which considers also presclerotic lesions) as well as proteinuria decreased slightly (although these decreases were not statistically significant).

General Histopathology

In accordance with previous studies of Masugi nephritis,[10,12] structural lesions developed quickly in all

Table 1. *Urine and Glomerular Data*

	U_{prot} (mg/day)	V_{glom} ($\times 10^6$ μm^3)	Glomerular injury		
			SGS (%)	GDI	FPF (%)
Control	11.7 ± 2.4	1.07 ± 0.32	0	0.5 ± 1.0	18.3 ± 3.6
Day 1	290.6 ± 60.3*	1.27 ± 0.12	0	28.5 ± 2.7	87.0 ± 6.8*
Day 3	386.1 ± 26.6*	1.65 ± 0.09	0	96.8 ± 5.1*†	92.5 ± 1.7*
Day 10	486.8 ± 112.6*	2.04 ± 0.16*†	3.6 ± 3.2	111.5 ± 17.1*†	83.0 ± 13.9*
Day 28	359.5 ± 65.4*	2.65 ± 0.28*†‡	28.8 ± 16.5*†‡§	97.5 ± 21.4*†	53.5 ± 3.5*†‡§

Values are mean ± SD. U_{prot}, urinary protein excretion; V_{glom}, average glomerular tuft volume; SGS, incidence of segmental glomerular sclerosis; GDI, glomerular damage index; FPF, fraction of foot process fusion.
*$P < 0.01$ *versus* control.
†$P < 0.01$ *versus* day 1.
‡$P < 0.01$ *versus* day 3.
§$P < 0.01$ *versus* day 10.

components of the tuft. Already 4 hours after serum application, widespread mesangiolysis and detachments of the endothelium from the GBM were seen (Figure 1). This led to an invasion of neutrophils and macrophages, which were seen sticking to inner capillary surfaces and in mesangial areas.

Beginning 3 days after serum application, endothelial and mesangial lesions were less frequently seen and were changing in character. The widespread fluid-filled spaces in the mesangium were replaced by compact extracellular matrices. Mesangial cells, tightly embedded into this matrix, appeared hypertrophied, being equipped with processes densely stuffed with microfilaments (best seen at late stages; see Figure 5). A more detailed analysis of these lesions will be presented elsewhere.

In podocytes, little structural damage was seen 4 hours after serum application. However, after one day podocyte lesions were widespread (Figure 1b) and propogated in the following days; finally, every podocyte appeared to be affected. The lesions included cell hypertrophy (also binucleated cells were observed), pseudocyst formation, and extensive foot process effacement (see below) as well as detachments from the GBM in varying degrees. The development of these lesions to segmental sclerosis will be described elsewhere. The present paper deals exclusively with the analysis of foot process effacement and its associated cytoskeletal changes.

Foot Process Effacement

The effacement of foot processes consists in the gradual simplification up to the total disappearance of the interdigitating pattern of podocyte foot processes paralleled by the shortening of the filtration slit. Foot process effacement in this model developed quickly. Compared with controls in which 82% of the outer capillary surface was covered by interdigitating foot processes, as early as 1 day after serum application only 13% of the outer GBM surface was still kept under cover by interdigitating foot processes (Table 1); the rest of the GBM was enwrapped by sheets of attenuated podocyte epithelium broadly adhering to the GBM. Thus, in only a small fraction of the outer capillary surface was the normal filtration route maintained. No significant changes were found after 3 to 10 days. However, 4 weeks after serum application, a significant improvement was observed; in almost 50% of the outer capillary surface, an interdigitating foot process pattern was found to be reconstituted.

The outspread portions of podocyte epithelium may smoothly attach to the outer surface of the GBM (Figures 1b and 2). Often, however, the interface between the GBM and the adhering podocyte sheets was very irregular, frequently exhibiting an undulating pattern (Figure 3).

The outstretched podocyte portions characteristically contain a prominent cytoskeleton. It appears to be fully developed as early as 3 days after injection of the serum and is best seen at those sites where these broad-based cell portions are smoothly attached to the GBM (Figure 2). In these cases a thick darkly stained belt paralleling the contours of cell attachment to the GBM is seen. This belt predominantly consists of densely arranged microfilaments with interspersed "densities."

In areas with an irregular attachment of the expanded podocyte portions, the cytoskeleton was also less uniformly arranged (Figure 3). In these cases the basal podocyte surface that faces the GBM should be imagined to contain variably shaped grooves and pits of different size. Microfilaments were densely accumulated in the prominences attaching to the GBM and more loosely arranged overlying the concavities. The microfilament bundles

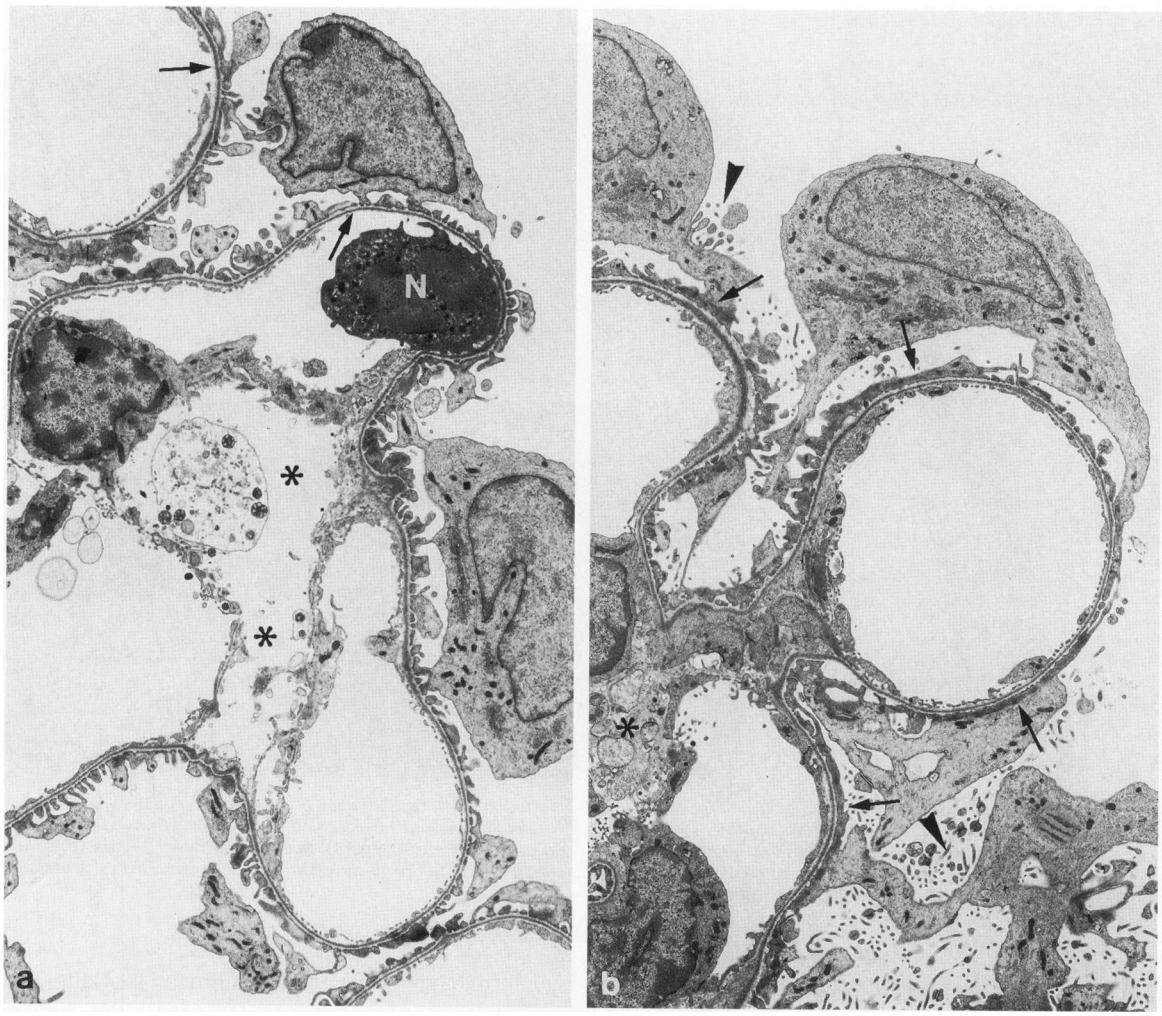

Figure 1. *Glomerular lesions, overviews* **a:** *Severe mesangiolysis* (**asterisks**) *and endothelial detachments* (**arrows**) *with a leukocyte* (*N, neutrophil*) *attaching to a denuded GBM area are observed 4 hours after serum injection. No apparent lesions in podocytes are seen.* **b:** *One day after serum injection, in addition to mesangiolysis* (**asterisk**) *and endothelial injury* (*not seen in this figure*), *widespread podocyte foot process effacement* (**arrows**) *is prominent. The continuous podocyte portions attaching to the GBM contain a darkly staining layer of microfilaments. Podocyte cell bodies exhibit numerous slender cytoplasmic projections* (**arrowheads**). *Masugi nephritis* (*MN*). *TEM,* **a** *and* **b** ×~3600.

within the prominences merge with the densities that were connected to the inner aspect of the basal cell membrane. Frequently, at the outer aspect of those areas, fibrous elements were seen interconnecting the cell membrane with the lamina densa of the GBM (Figure 3b).

In grazing sections through this microfilament layer (Figures 2b and 4) a specific pattern can clearly be recognized. Microfilaments extend into all directions establishing a three-dimensional network. At regular intervals, densities are seen to which the microfilaments connect. These densities obviously allow the interconnection of microfilaments arriving from various directions. At the interface of this basally located microfilament layer toward the cell body cytoplasm, close spatial relationships with intermediate filaments and microtubules were seen (Figure 4 b).

At day 28, an interdigitating foot process pattern had recovered at many sites (Figures 5 and 6). Different degrees of restitution were seen. However, even in areas of the most advanced reconstitution the interdigitating pattern was much less regular than the one seen in controls. Individual foot processes were quite different in width and irregular in shape but clearly separated by filtration slits of apparently normal width (Figure 6). They contained microfilaments in variable density and arrangement; dense bodies located in the midst of microfilament bundles as well as associated with the basal cell membrane were still prominent. In addition, numerous multivesicular bodies were encountered within these irregularly shaped foot processes.

The interface of these newly established foot processes to the underlying GBM was quite irregular, as

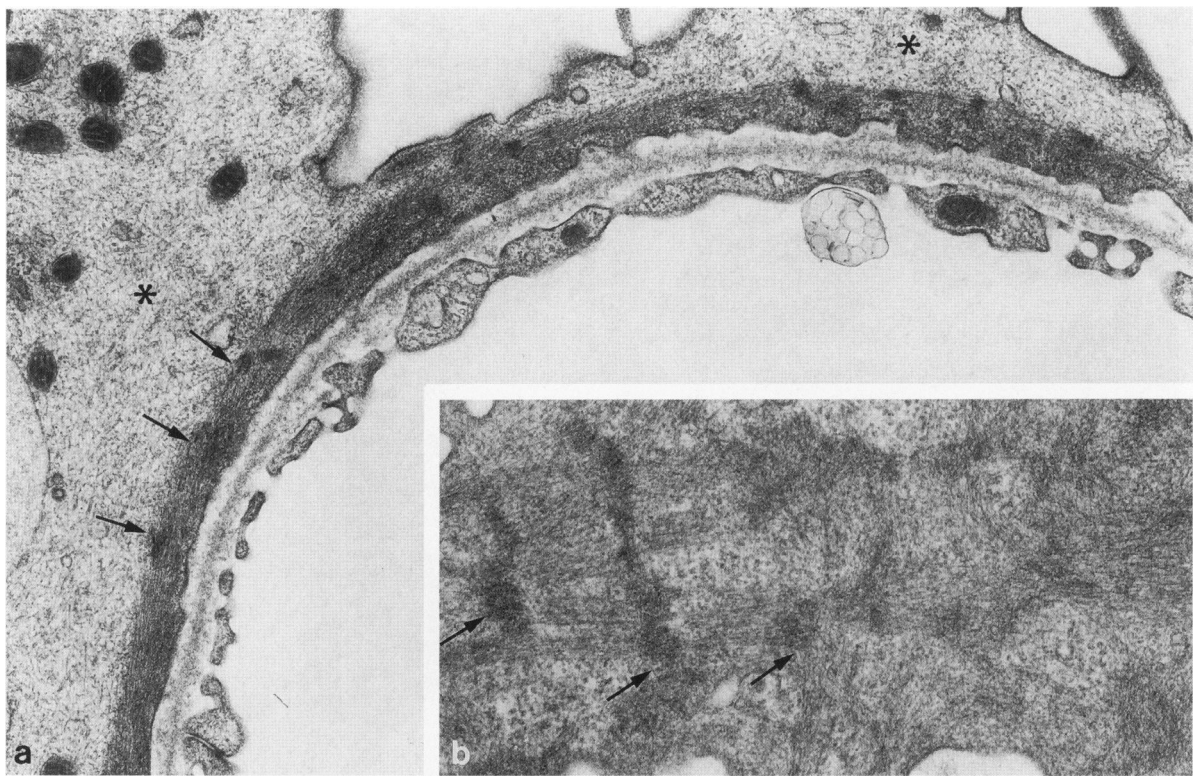

Figure 2. *Foot process effacement in an area of smooth podocyte attachment to the GBM.* (a) *Overview of glomerular capillary wall. The basal podocyte cytoplasm contains a prominent dark staining belt made up of a microfilamentous network with interspersed dense bodies* (arrows). *Elsewhere, the podocyte cytoplasm includes abundant microtubules and intermediate filaments* (asterisks). *Note the intact endothelium.* (b) *Grazing section through the basal microfilament layer. Microfilament bundles extending into virtually all directions are interconnected at dense bodies* (arrows). *MN, day 30. TEM,* (a) ×~*23000,* (b) ×~*38000.*

well. The interposed spaces (probably corresponding to former disconnections) were filled with extracellular matrices in variable amounts similar in appearance and density to lamina densa material. At some places the newly formed material appeared as a second dense layer arranged on top of the original lamina densa, whereas at other places a fairly homogenous elaboration including the merging with the original lamina densa of the GBM was seen.It appeared that a more complete filling of these spaces with such material was associated with a more advanced reconstitution of an interdigitating foot process pattern.

Immunocytochemical Results

The distribution of F-actin, α-actinin, and pp44 was examined by immunofluorescence techniques. Control rats revealed the well known distribution of these proteins[9,13] (Figure 7). The staining for F-actin was more intense in the mesangium than in the peripheral capillary wall (reflecting at the latter site the occurrence in podocyte foot processes). Staining for α-actinin was seen in the mesangium and the capillary wall, exhibiting a dotted pattern at the latter site. pp44 staining was recognized only in the capillary wall with enhancements in the angle regions between neighboring capillaries.

In Masugi nephritis, the distribution and density of these proteins were changed. There was a drastic increase of F-actin staining in the peripheral capillary wall (reflecting podocyte staining), most remarkable on day 3 and day 10 but clearly maintained up to day 28 (Figure 7a). In contrast, F-actin staining in the mesangial regions was markedly decreased or almost absent in the early phase of the disease (day 1 and day 3); thereafter a mesangial staining recovered and was quite prominent on day 28. Thus, on day 28, F-actin staining was strong in both mesangium and podocytes (Figure 7a).

Compared with controls, staining for α-actinin increased considerably in Masugi nephritis (Figure 7b). The capillary wall stained brightly in a dotted-line pattern throughout the course of the disease. The pattern of pp44 staining (paralleling the capillary wall) did not change, but its intensity was considerably enhanced up to day 28 (Figure 7c).

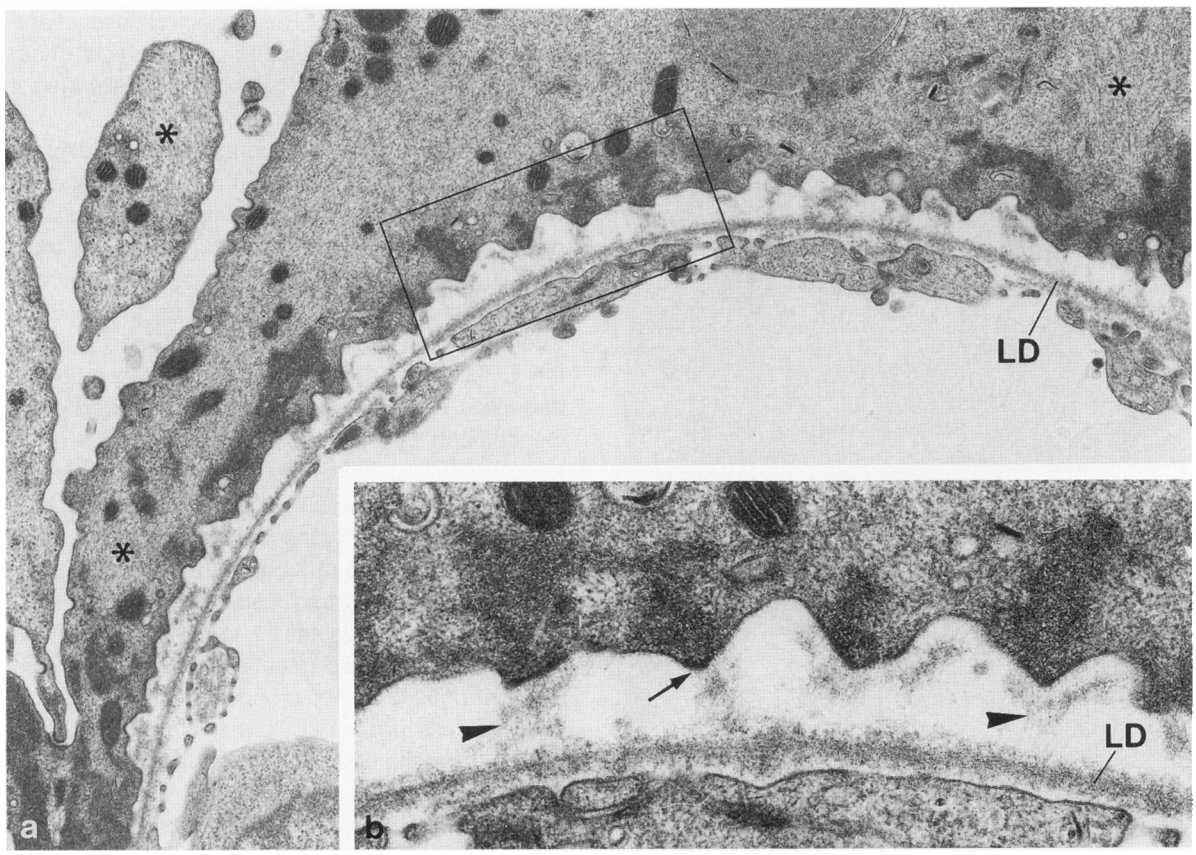

Figure 3. *Foot process effacement in an area with irregular cell-GBM-interface.* (**a**) *Overview of capillary wall. The basal podocyte cytoplasm contains a prominent skeleton consisting of microfilaments that are accumulated in the cell protrusions connected to the lamina densa* (*LD*) *of the GBM. Within the cytoplasm overlying the concavities microfilaments are less densely arranged. In other parts of the podocyte cytoplasm* (**asterisks**) *the cytoskeleton is quite differently composed of microtubules and microfilaments. The endothelium is intact.* (**b**) *Enlarged area of* (**a**). *The dense microfilamentous cytoskeleton within the protrusion attaches to densities associated with the basal cell membrane* (**arrow**). *The ample space between the basal podocyte surface and the lamina densa of the GBM is quite irregular in width and contains connections between basal podocyte protrusions and the lamina densa* (**arrowheads**); *otherwise this space appears mostly empty. MN, day 10. TEM,* (**a**) ×~*14000,* (**b**) ×~*37000.*

By immunogold techniques labeling for actin, α-actinin and pp44 were found in controls in patterns known from previous work[9,13] (Figure 8). In Masugi nephritis gold labeling for actin in podocytes was diffusely distributed throughout the hypertrophied microfilament network (Figure 9a),whereas α-actinin was found to accumulate in dark areas of the network (Figure 9b) corresponding to the densities seen in TEM. Gold labeling for pp44 was intense throughout the cytoskeletal belt (Figure 9c) complemented by focal enhancements.

Discussion

The terms foot process effacement or foot process fusion designate a phenomenon consisting in the simplification and, eventually, in the almost total disappearance of an interdigitating pattern of podocyte foot processes. Concomitantly, the filtration slit is drastically shortened, reduced to the serpentine cell borders between neighboring podocytes. Experimentally, fusion of foot processes has been observed to occur very quickly in response to infusion of highly cationic compounds[14] that destroy the negative surface charge of podocytes. Cytochalasins[15] as well as removal of Ca^{++}[16] have been shown to interfere with this process, suggesting that the fusion of foot processes depends on the contraction of the microfilament system in the foot processes.

The present study does not deal with these acute events. Instead, this study analyzes foot process effacement in its accomplished elaboration as it is generally encountered in a variety of experimental as well as human glomerulopathies. These include puromycin aminonucleoside nephrosis,[17–19] Heyman nephritis,[20,21] DOCA-salt hypertension,[22,23] 5/6 nephrectomy,[24,25] FSGS development after UNX in young rats,[1] after long-term treatment with FGF-2[26] and in Milan normotensive rats.[27] In human biopsies as well as autopsies, effacement of foot processes is especially common in minimal change nephropathy,[28–30] membranous nephropathy,[31] and focal glo-

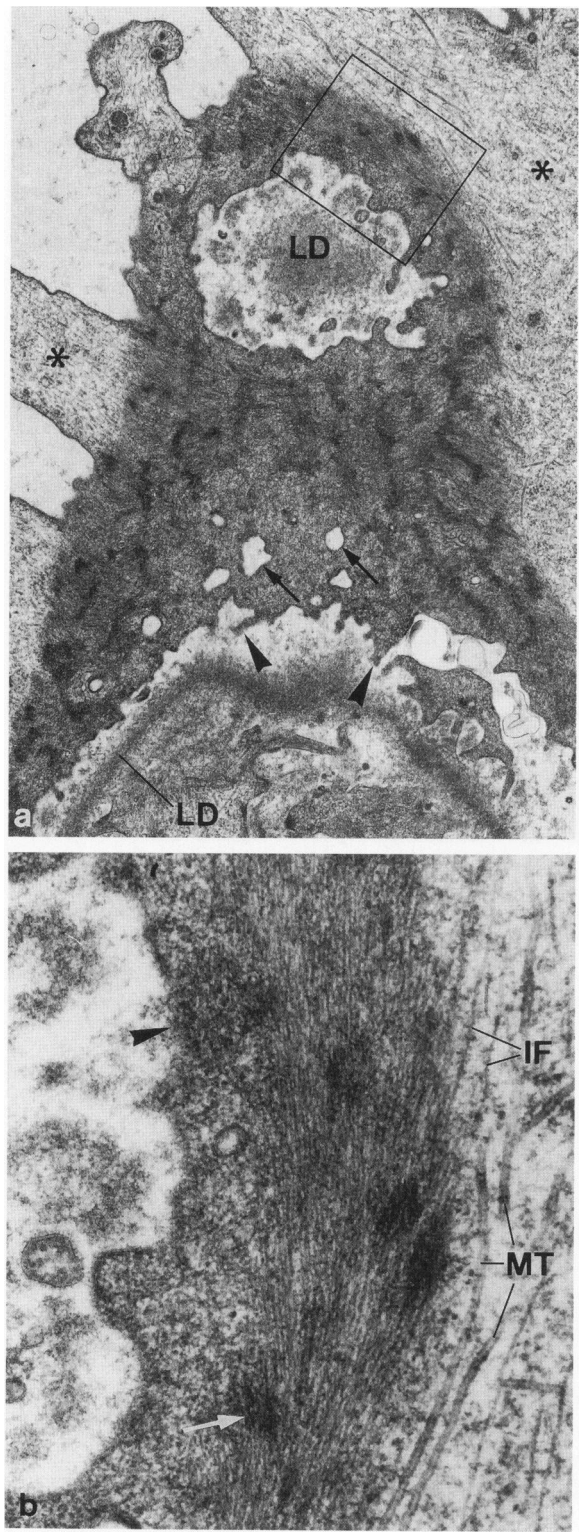

Figure 4. *Cytoskeleton in basal podocyte cytoplasm.* (**a**) *Grazing section through capillary wall; the lamina densa* (*LD*) *of the GBM is cut at two sites. The dense microfilament network appears as a homogenous layer sharply separated from the adjacent pale staining cytoplasm elsewhere in the cell* (**asterisks**). *The basal cell surface is irregular with grooves* (**arrows**) *and protrusions extending into the space that may be considered as a widened lamina rara externa of the GBM. The microfilament network contains regularly distributed dense bodies.* (**b**) *Enlarged area of* (**a**). *Within the basal microfilament layer individual filaments* (*6–8 nm thick*) *can easily be distinguished. They are anchored in dense bodies, which are either located in the midst of the network* (**arrow**) *or are associated with the basal cell membrane* (**arrowhead**). *At the interface to the cell body cytoplasm an association of microfilaments with intermediate filaments* (*IF*) *and microtubules* (*MT*) *is seen. MN, day 10. TEM,* (**a**) *9300,* (**b**) *×~47500.*

merulosclerosis.[30,32,33] Thus, foot process effacement represents a stereotyped change in cell shape on which podocytes fall back when challenged in certain pathological situations.

When comparing the elaboration of the outspread sheets of podocyte epithelium in the present study with that in most other models (just mentioned above) a difference must be mentioned. In those models the expanded podocyte portions generally attach smoothly to the outer surface of the GBM, whereas in Masugi nephritis the interface between the GBM and the outspread podocyte portions is frequently very irregular with variably shaped prominences and concavities in the basal surface of the adhering cell portions. In early stages of the disease these concavities appear empty; later they are filled with basement membrane-like material (see below). It is known that anti-rat-GBM sera (used to induce Masugi nephritis) contain antibodies that react with a β_1-integrin on podocytes.[34] Thus, compared with other models of FSGS (mentioned above), a particular component of foot process effacement in Masugi nephritis apparently is that the attachment of podocytes to the GBM may be impaired by antibodies that interfere with interconnecting integrins.[35] The pattern of incomplete disconnections of podocytes from the GBM as seen in this study would fit with partial but widespread impairments of the integrin connections.

Cytoskeletal Changes

Foot process effacement is regularly associated with conspicuous changes in the cytoskeleton, quantitatively as well as qualitatively. The increase in microfilaments together with the elaboration as a broad belt attaching to the basal cell membrane has previously been noted[1,23,30,36,37]; however, a detailed analysis is so far lacking. This newly established cytoskeletal mat consists of densely arranged microfilaments and exhibits a high degree of organization. Within this mat, microfilaments, frequently elaborated as stress fibers, run in virtually all directions. At regular intervals, densities are interspersed, which obviously serve as anchor points for the microfilament bundles; α-actinin staining is most intensive in these densities. Thus, from their structural appear-

Figure 5. *Reconstitution of an interdigitating foot process pattern. Overview of a peripheral part of a lobule with four capillary profiles.*[1–4] *The center between the capillaries is made up of solidified mesangial tissue consisting of extensively branched mesangial cells* (asterisks) *and a compact matrix. The peripheral capillary wall is decorated by a coarse pattern of interdigitating foot processes that are quite irregular in shape. Podocyte cell bodies contain many dark staining granules* (star), *probably lysosomal in character. MN, day 28. TEM, ×~2000.*

ance as well as from the accumulation of α-actinin it may be concluded that these densities correspond to the dense bodies in smooth muscle cells,[38] which serve as crosslinkers for microfilaments.[39] Such a function would make sense here as well. Microfilaments approach these dense bodies from all directions. If we assume that the direction of a microfilament bundle reflects a possible tension line, mechanical strain from virtually all directions would be interconnected in these dense bodies.

In a recent study of PAN-nephrosis[40] the dense and uniform distribution of actin labels seen by immunogold labeling in the basal podocyte cytoplasm has been interpreted as showing an increase in available epitopes on disaggregated actin due to a direct toxic effect of PAN to podocytes. In our material in Masugi nephritis, the increased actin labeling corroborates with increased phalloidin staining (specific for filamentous actin) and remodeling of the cytoskeleton microfilaments into a highly organized texture. In addition, labeling for pp44 (which represents a characteristic cytoskeletal protein of differentiated podocytes[9]) was maintained and increased in intensity. Thus, foot process effacement in Masugi nephritis appears as an adaptive process associated with hypertrophy and reorganization of the basal cytoskeleton. As indicated from cytoskeletal changes at other sites,[41] impairments of the integrin connections might play an important role in the reorganization of the podocyte cytoskeleton in Masugi nephritis.

The pattern of foot process interdigitation has been interpreted as serving for two functions:[42] first, like pericytes elsewhere, to counteract the elastic distension of the capillary wall making use of contractile apparatus of the foot processes and second, to provide a paracellular route for convective water flow by leaving a filtration slit between the foot processes. In Masugi nephritis, as well as in other situations going along with foot process effacement (see above) the challenge to podocytes to counteract the distension of the capillary wall is probably increased. Such an increase may be due to various factors including a rise in glomerular capillary pressure (known to occur in Masugi[43,44]), impairment of the GBM decreasing its inherent stability and the strength of its contacts to podocytes, and loss or impairment of mesangial support; all three factors might be effective in Masugi nephritis. From this point of view, hypertrophy of the contractile apparatus in foot process effacement may be seen as an adaptive change to allow a more effective counteraction of the distending forces exerted to the capillary wall. On the other hand, based on the loss of filtration slits, foot process effacement comprises the specific permeability of the filtration barrier as indicated by observations that foot process effacement strongly correlates with reductions in glomerular fil-

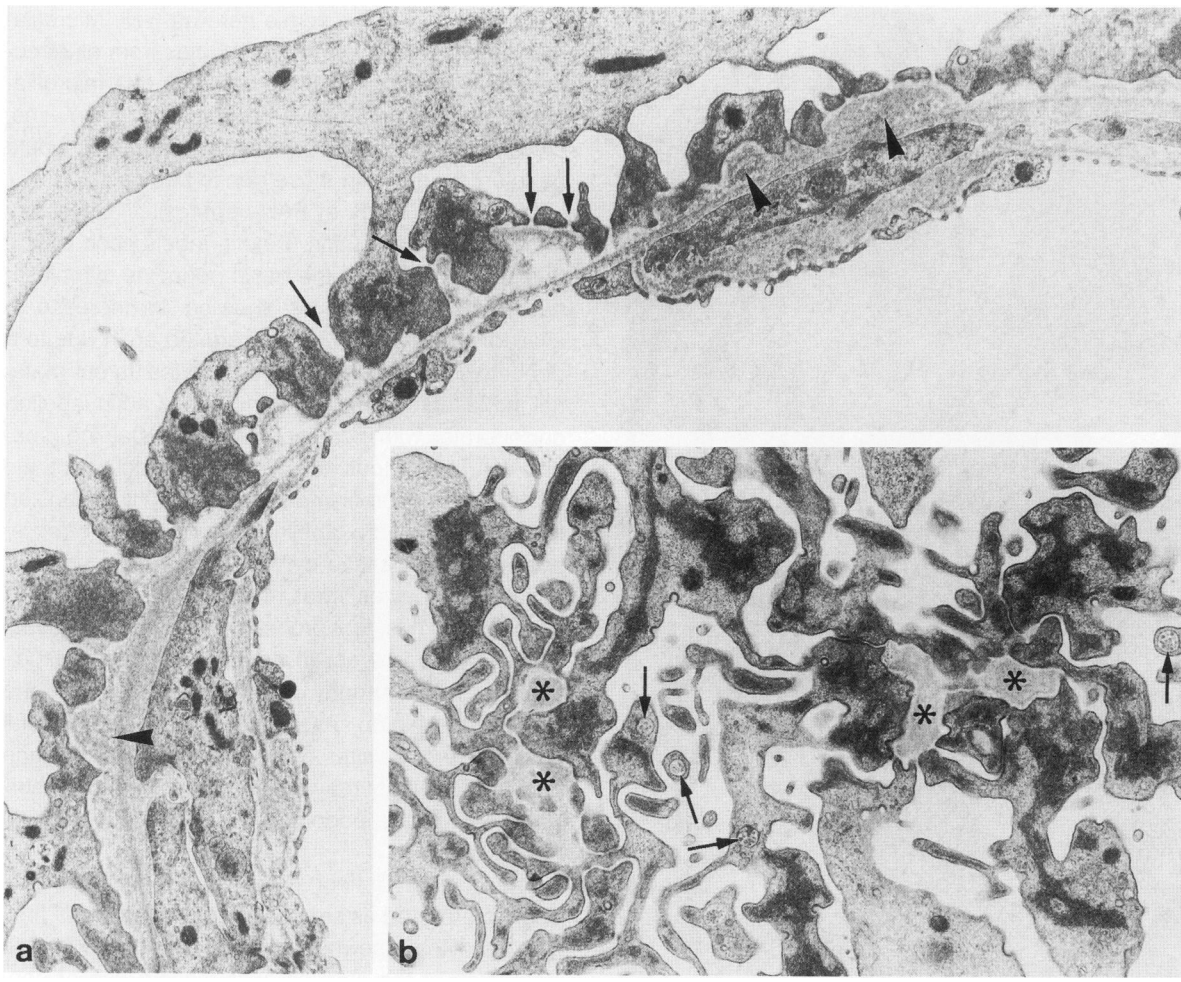

Figure 6. *Capillary wall with reconstituted foot process interdigitation.* (a) *Peripheral capillary wall decorated by coarse foot processes. Individual foot processes filled by a densely arranged cytoskeleton are quite irregular in shape, but separated by filtration slits of apparently normal width* (arrows). *The interface between the sole plates of the foot processes and the lamina densa of the GBM consists of an irregular space, which at some places is filled by an extracellular matrix corresponding in its density to lamina densa material* (arrowheads). (b) *Grazing section through the podocyte-GBM-junction of a capillary wall. The GBM is touched at several sites* (asterisks). *Irregularly shaped processes (representing intermediates in the remodelling process of foot processes) make contact with the GBM. They contain coarse plaques of microfilament assemblies and many multivesicular bodies* (arrowheads). *MN, day 28. TEM,* (a) ×~10800, (b) ×~10800.

tration rate underlain by reductions of the ultrafiltration coefficient, Kf.[45,46]

Reconstitution of a Foot Process Pattern

The reconstitutive process begins late; at day 10 after planting the injury, no signs of foot process recovery were encountered. At the end of the study, on day 28 the beginning of a reorganization of an interdigitating foot process pattern is clearly seen. Roughly 50% of the outer capillary surface was redecorated with interdigitating foot processes. Thus, the repair process clearly had begun but was far from being complete.

Several aspects of these reconstitution processes are worth discussion. First, the newly established pattern of interdigitating foot processes is much less symmetrically organized than the pattern seen in controls. The foot processes are quite variable in size and shape and contain variable amounts of a cytoskeleton. It appears as if the hypertrophied cytoskeleton of the outspread podocyte portions has

Figure 7. *Immunostaining for F-actin* (a), *α-actinin* (b), *and pp44* (c) *In controls, F-actin stains dominantly in mesangial areas* (a1). *In Masugi nephritis, at day 3 F-actin staining is prominent in capillary walls* (a2). *In later stages of MN (day 10 and 28) the capillary wall as well as the mesangium are strongly positive for F-actin, the mesangium is most densely stained at day 28* (a4). *Staining for α-actinin* (b)) *is already drastically increased at day 3* (b2) *when compared to control* (b1). *A prominent α-actinin staining is maintained at later stages of MN* (b3 *and* b4). *Staining for pp44* (c) *is exclusively seen in capillary walls and is considerably increased in MN* (c2-c4) *compared to controls* (c1). *1) Control, 2) MN day 3, 3) MN day 10, and 4) MN day 28. LM, ×~150.*

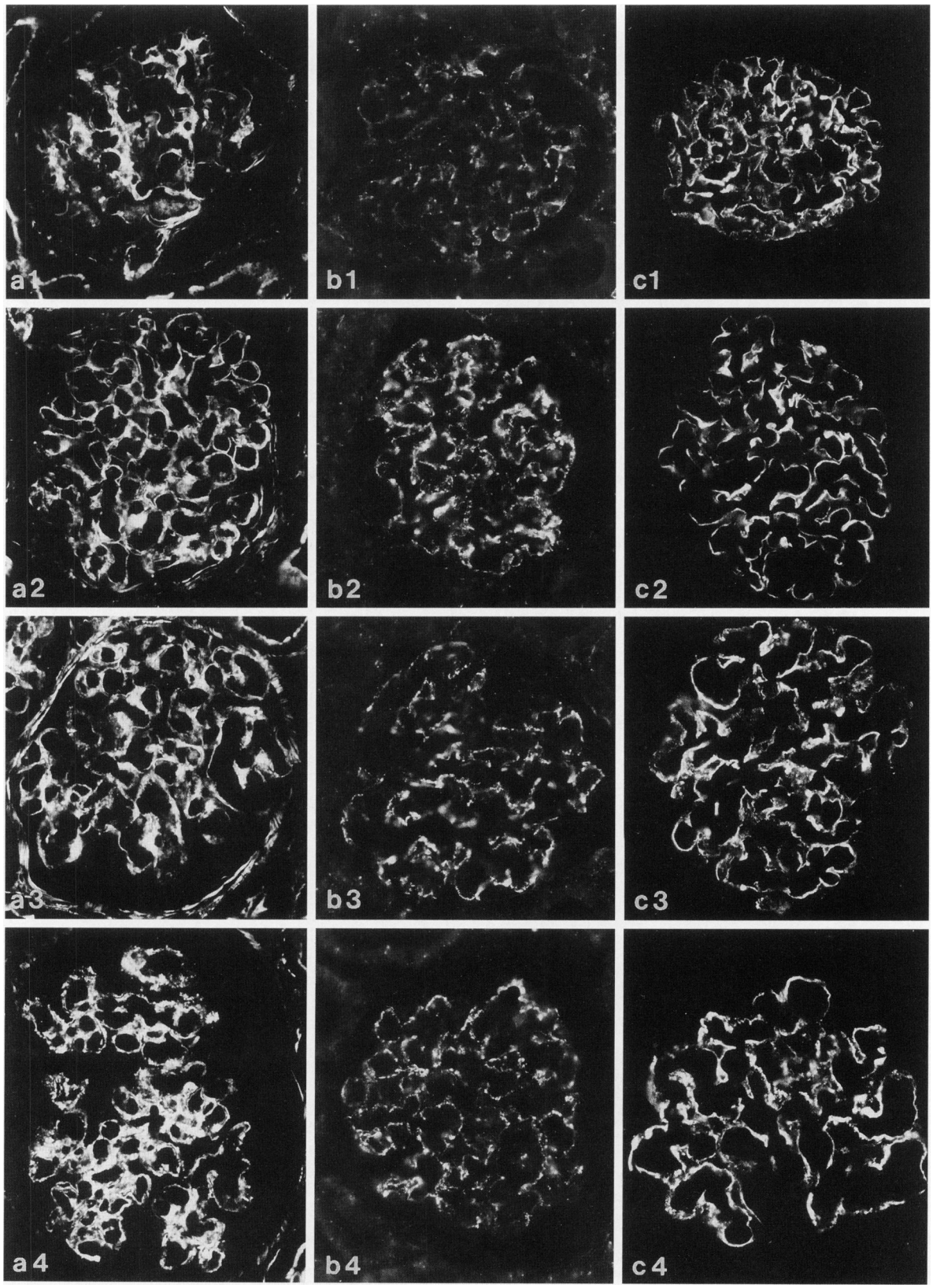
a1
b1
c1
a2
b2
c2
a3
b3
c3
a4
b4
c4

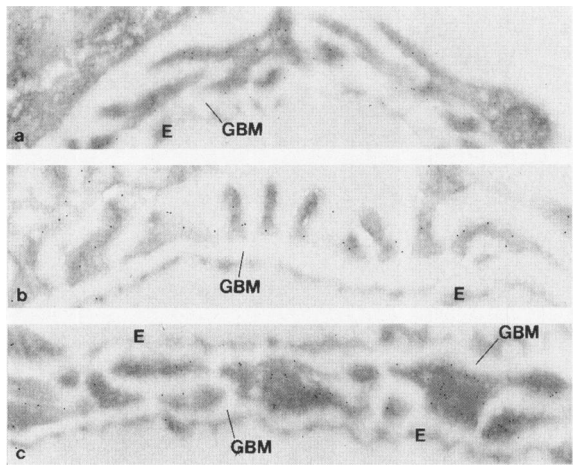

Figure 8. *Immunogold labeling for actin, α-actinin and pp44 in controls Gold labels for actin* (a), *α-actinin* (b) *and pp44 are found in podocyte foot processes. More heavy labelling with pp44 is seen in larger processes filling the niches between neighboring capillaries thereby interconnecting opposing parts of the GBM* (c). *These distributions fully correspond to findings in previous studies.*[9,13] *Control rats. P, podocyte. TEM,* (a-c) ×~20000.

been partitioned into the newly developing processes and is now undergoing dissolution. The many multivesicular bodies seen in these areas may indicate an increased catabolism. Thus the reestablishment of an interdigitating foot process pattern appears to include quite extensive decomposing processes.

Second, podocytes synthesize new extracellular material (appearing identical to lamina densa material) with which the defects between the podocytes and the GBM are filled. A similar process has previously been described in heroin-associated nephropathy.[32] The synthesis of such material is reflected in the apparent enrichment of endoplasmic reticulum and Golgi fields in the podocyte cytoplasm. This process may be interpreted as to restore fixation of podocytes to the GBM. Because the attachment of foot processes to the GBM is critically based on integrin connections (which probably had been directly impaired by antibodies contained in the "Masugi serum"; see above), repair of integrin connections appears pivotal for reaffixation. Thus, as a very first precondition of foot process restitution podocytes need firm contacts to the GBM.

Third, the damaging effect of the serum was initially seen at the mesangium and the endothelium (widespread mesangiolysis and endothelial detachments). At day 28 these lesions had undergone widespread repair. Newly produced mesangial matrices have apparently re-established firm connections between mesangial cells and the GBM (as seen in Figure 5). As discussed previously,[47] this solidified form of mesangial expansion may be regarded as successful repair in the sense that the GBM has been reattached to the mesangium. Recovery of a foot process pattern was generally seen at those sites. Thus, in addition to intact podocyte-GBM connections reconstitution of an interdigitating foot process pattern appears to be dependent on a preceding re-establishment of mesangial support function. Further studies are necessary to understand this process in more detail.

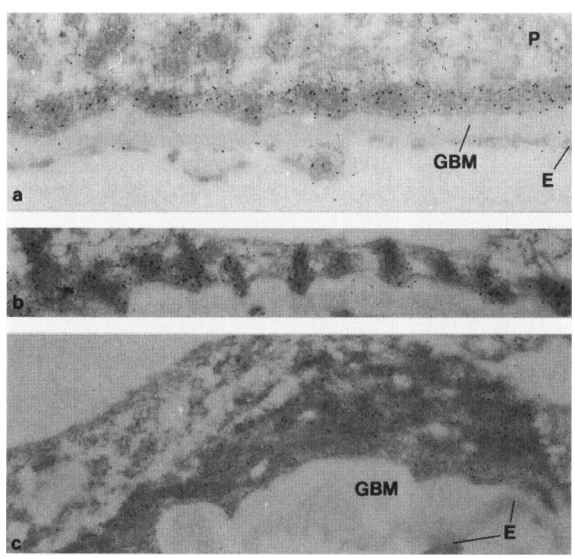

Figure 9. *Immunogold labelling of podocytes in Masugi nephritis* (a) *Labelling for actin. The basal skeletal belt of fused podocyte portions exhibits a dense and regular distribution of gold particles.* (b) *Labelling for α-actinin. Gold particles are accumulated in the densities of podocyte protrusions attached to the GBM.* (c) *Labelling for pp44. A dense pattern of particles is seen throughout the basal cytoskeletal network, demonstrated here in a grazing section. MN, day 10. E, endothelium; P, podocyte. TEM,* (a) ×~15000, (b) ×~19000 *and* (c) ×~16000.

Acknowledgments

We thank Ms. Hiltraud Hosser, Ms. Bruni Hähnel, and Ms. Ingrid Hartmann for technical assistance, Ms. Ingrid Ertel for photographic work, and Ms. Marlis Schuchardt for secretarial help.

References

1. Nagata M, Kriz W: Glomerular damage after uninephrectomy in young rats. II. Mechanical stress on podocytes as a pathway to sclerosis. Kidney Int 1992, 42:148–160
2. Davies DJ, Brewer DB, Hardwicke J: Urinary proteins and glomerular morphometry in protein overload proteinuria. Lab Invest 1978, 38:232–243
3. Cho CR, Lumsden CJ, Whiteside CI: Epithelial cell detachment in the nephrotic glomerulus: a receptor cooperativity model. J Theor Biol 1993, 160:407–426
4. Kondo Y, Akikusa B: Chronic Masugi nephritis in the

rat: an electron microscopic study on evolution and consequences of glomerular capsular adhesions. Acta Pathol Jpn 1982, 32:231–242
5. Sakai T, Kriz W: The structural relationship between mesangial cells and basement membrane of the renal glomerulus. Anat Embryol 1987, 176:373–386
6. Kaissling B, Kriz W: Variability of intercellular spaces between macula densa cells: a transmission electron microscopic study in rabbits and rats. Kidney Int 1982, 22(Suppl 12):S9-S17
7. Shirato I, Sakai T, Fukui M, Tomino Y, Koide H: Widening of capillary neck and alteration of extracellular matrix ultrastructure in diabetic rat glomerulus as revealed by computer morphometry and improved tissue processing. Virchows Arch A 1993, 423:121–129
8. Weibel, ER: Stereological Methods: Practical Methods for Biological Morphometry. London, Academic Press, 1979
9. Mundel P, Gilbert P, Kriz W: Podocytes in glomerulus of rat kidney express a characteristic 44 kD protein. J Histochem Cytochem 1991, 39:1047–1056
10. Kondo Y, Shigematsu H, Okabayashi A: Cellular aspect of rabbit Masugi nephritis. III. Mesangial changes. Lab Invest 1976, 34:363–371
11. Nahas AME: Masugi nephritis: a model for all seasons. Experimental and Genetic Rat Models of Chronic Renal Failure. Edited by N Gretz, M Strauch. Basel, Karger, 1993, pp 49–67
12. Kühn K, Ryan GB, Hein SJ, Galaske RG, Karnovsky MJ: An ultrastructural study of the mechanism of proteinuria in rat nephrotoxic nephritis. Lab Invest 1977, 36:375–387
13. Drenckhahn D, Franke RP: Ultrastructural organization of contractile and cytoskeletal proteins in glomerular podocytes of chicken, rat, and man. Lab Invest 1988, 59:673–682
14. Seiler MR, Rennke HG, Venkatachalam MA, Cotran RS: Pathogenesis of polycation-induced alteration (fusion) of glomerular epithelium. Lab Invest 1977, 36:48–61
15. Andrews PM: Cationized ferritin binding to anionic surfaces in normal and aminonucleoside nephrotic kidneys. Am J Anat 1981, 162:89–106
16. Kerjaschki D: Polycation-induced dislocation of slit diaphragms and formation of cell junctions in rat kidney glomeruli: the effects of low temperature, divalent cations, colchicine, and cytochalasin B. Lab Invest 1978, 39:430–440
17. Farquhar MG, Palade GE: Glomerular permeability. II. Ferritin transfer across the glomerular capillary wall in nephrotic rats. J Exp Med 1961, 114:699–715
18. Ryan GB, Karnovsky MJ: An ultrastructural study of the mechanisms of proteinuria in aminonucleoside nephrosis. Kidney Int 1975, 8:219–232
19. Messina A, Davies DJ, Dillane PC, Ryan GB: Glomerular epithelial abnormalities associated with the onset of proteinuria in aminonucleoside nephrosis. Am J Pathol 1987, 126:220–229
20. Heymann W, Hackel DB, Harwood S, Wilson SGF, Hunter JPL: Production of nephrotic syndrome in rats by Freunds adjuvants and rat kidney suspensions. Proc Soc Exp Biol Med 1959, 100:660–664
21. Kerjaschki D: Molecular pathology of membranous nephropathy. Kidney Int 1992, 41:1090–1105
22. Dworkin LD, Hostetter TH, Rennke HG, Brenner BM: Hemodynamic basis for glomerular injury in rats with desoxycorticosterone-salt hypertension. J Clin Invest 1984, 73:1448–1461
23. Kretzler M, Koeppen-Hagemann I, Kriz W: Podocyte damage is a critical step in the development of glomerulosclerosis in the uninephrectomised-desoxycorticosterone rat. Virchows Arch A 1994, 452:181–193
24. Shimamura T, Morrison AB: A progressive glomerulosclerosis occurring in partial five-sixths nephrectomized rats. Am J Pathol 1975, 79:95–106
25. Faraj AH, Morley AR: Remnant kidney pathology after five-sixth nephrectomy in rat. II. Electron microscopy study. APMIS 1993, 101:83–90
26. Kriz W, Hähnel B, Rösener S, Elger M: Long-term treatment of rats with FGF-2 results in focal segmental glomerulosclerosis. Kidney Int 1995, 48:1435–1450
27. Brandis A, Bianchi G, Reale E, Helmchen U, Kuhn K: Age-dependent glomerulosclerosis and proteinuria occurring in rats of the Milan normotensive strain and not in rats of the Milan hypertensive strain. Kidney Int 1986, 55:234–243
28. Farquhar MG, Vernier RL, Good RA: An electron microscope study of the glomerulus in nephrosis, glomerulonephritis, and lupus erythematosus. J Exp Med 1957, 106:649–660
29. Olson JL: The nephrotic syndrome. Pathology of the Kidney. Edited by RH Heptinstall. Boston, Little Brown and Co., 1992, pp 839–844
30. Nadasdy T, Silva FG, Hogg RI: Minimal change nephrotic syndrome: focal sclerosis complex. Renal Pathology. Edited by CC Tisher, BM Brenner. Philadelphia, JB Lippincott, 1994, pp 330–389
31. Ehrenreich T, Churg J: Pathology of membranous nephropathy. Pathol Annu 1968, 3:145–186
32. Grishman E, Churg J: Focal glomerular sclerosis in nephrotic patients: an electron microscopic study of glomerular podocytes. Kidney Int 1975, 7:111–122
33. Velosa JA, Donadio JV, Holley KE: Focal sclerosing glomerulonephropathy: a clinicopathologic study. Mayo Clin Proc 1975, 50:121–133
34. O'Meara YM, Natori Y, Minto AW, Goldstein DJ, Manning EC, Salant DJ: Nephritogenic antiserum identifies a β1-integrin on rat glomerular epithelial cells. Am J Physiol 1992, 262:F1083-F1091
35. Adler S: Integrin receptors in the glomerulus: potential role in glomerular injury. Am J Physiol 1992, 262:F697-F704
36. Olson JL, Heptinstall RH: Biology of disease: nonimmunologic mechanisms of glomerular injury. Lab Invest 1988, 59:564–578
37. Fries JW, Sandstrom DJ, Meyer TW, Rennke HG: Glomerular hypertrophy and epithelial cell injury modulate

progressive glomerulosclerosis in the rat. Lab Invest 1989, 60:205–218
38. Lemanski L, Paulson D, Hill GS, Davis LA, Riles LC, Lim SS: Immunoelectron microscopic localization of α-actinin on Lowicryl-embedded thin-sectioned tissues. J Histochem Cytochem 1985, 33:515–522
39. Critchley, DR: α-Actinin. Guidebook to the Cytoskeletal and Motor Proteins. Edited by T Kreis, R Vale. Oxford, Oxford University Press, 1993, pp 22–23
40. Whiteside CI, Cameron R, Munk S, Levy J: Podocytic cytoskeletal disaggregation and basement-membrane detachment in puromycin aminonucleoside nephrosis. Am J Pathol 1993, 142:1641–1653
41. Fox JEB: Transmembrane signaling across the platelet integrin glycoprotein IIb-IIIa. Ann NY Acad Sci 1994, 714:75–87
42. Kriz W, Elger M, Mundel P, Lemley KV: Structure-stabilizing forces in the glomerular tuft. Am J Nephrol 1995, 5:1731–1739
43. Blantz RC, Wilson B: Acute effect of antiglomerular basement membrane antibody on the process of glomerular filtration in the rat. J Clin Invest 1976, 58:899–911
44. Maddox DA, Bennet CM, Deen WM, Glassock RJ, Knutson D, Daugharty TM, Brenner BM: Determinants of glomerular filtration in experimental glomerulonephritis in the rat. J Clin Invest 1975, 55:305–318
45. Drumond MC, Kristal B, Myers BD, Deen WM: Structural basis for reduced glomerular filtration capacity in nephrotic humans. J Clin Invest 1994, 94:1187–1195
46. Guasch A, Myers BD: Determinants of glomerular hypofiltration in nephrotic patients with minimal change nephropathy. J Am Soc Nephrol 1994, 4:1571–1581
47. Lemley KV, Elger M, Koeppen-Hagemann I, Kretzler M, Nagata M, Sakai T, Uiker S, Kriz W: The glomerular mesangium: capillary support function and its failure under experimental conditions. Clin Invest 1992, 70: 843–856